Journal of Thermal Analysis, Vol. 47 (1996) 697-713

THERMAL DEGRADATION OF POLY(VINYL BUTYRAL) IN ALUMINA, MULLITE AND SILICA COMPOSITES

*T. C. K. Yang, W. H. Chang and D. S. Viswanath**

Department of Chemical Engineering, University of Missouri-Columbia Columbia, MO 65211, USA

(Received July 21, 1995; revised form January 3, 1996)

Abstract

Thermal degradation of poly(vinyl butyral) (PVB) and its mixtures with alumina, mullite and silica was investigated by non-isothermal thermogravimetry in the temperature range of 323 to 1273 K. The analysis of the data was carried out using a three-dimensional diffusion model. Results showed that the kinetic parameters (activation energy and pre-exponential factor) of the PVB degradation are different for polymer alone, and ceramic/polymer composites. The overall weighted mean apparent activation energy showed an increasing reactivity in the order of PVB<alumina + PVB<mullite + PVB<silica + PVB. This shows that the acidic and basic surface characteristics of the ceramics promote the thermal degradation of PVB and, the more acidic silica affects the degradation more than mullite and alumina. The effect of pellet compression pressure in the range of 4000 to 8000 psig is also investigated.

Keywords: ceramics, kinetic analysis, polymer, PVB, thermal degradation

Introduction

A knowledge of kinetic analysis is necessary to investigate quantitatively the thermal decomposition behavior of organic polymers which are used extensively in ceramic processing. Even though the organic polymer binders play a temporary role in the manufacture of various ceramic components such as multichip modules, the thermal degradation of binders determines the quality of the ceramic substrate. It has been reported that incomplete binder burnout would retard densification rates and limit the final density achieved. In addition, the residual carbon left behind after thermal degradation affects optical, electrical and mechanical properties of the substrate. The residual carbon in excess of 50

* To whom all correspondence should be addressed.

0368–4466/96/ $ 5.00

John Wiley & Sons, Limited
Chichester

to 100 ppm would decrease the density and also affect many substrate properties like flexural strength, breakdown voltage [1] and dielectric constant [2]. In order to optimize the binder removal processes, some attention has been paid to studies such as polymer degradation mechanism [3–5], interactions of ceramics and binders [6–8], and effect of processing variables [9]. However information on kinetics of thermal degradation is limited.

Literature review

There has been a considerable amount of work on the thermal degradation of polymers in ceramic surfaces. Parker *et al.* [10] studied the mobility of polymer in the presence and absence of alumina and plasticizer. Bakht [4] studied the thermal degradation of PVB copolymers in the temperature range of 473 to 723 K. The PVB used had different degrees of vinyl butyral substitution. Thermal Volatilization Analysis (TVA), Thermogravimetric Analysis (TG) and Infrared Spectroscopy (IR) were used to investigate the composition of the volatile products formed due to the decomposition of PVB. Bakht observed the products of thermal degradation of PVB to be mainly water and butyraldehyde. He proposed both a free radical mechanism and a molecular elimination mechanism to interpret the formation of butyraldehyde.

Sacks *et al.* [7] carried out a series of studies on the degradation mechanisms and pyrolysis behavior of PVB and acrylic polymers (i.e. poly(methyl methacrylate) and poly(methacrylic acid)). Degradation experiments were carried out for polymers alone and for polymer–ceramic mixtures in nitrogen or oxygen atmospheres. They found that the mechanism of thermal degradation of poly(methyl methacrylate) to be depolymerization, and furthermore they observed that the reaction was accelerated by the presence of oxygen (thermal-oxidative degradation). In the case of poly(methyl methacrylate) and alumina mixture, a surface reaction between the polymer and the ceramic was indicated by Fourier transform infrared spectroscopy (FTIR) and gas chromatography (GC) results, but not in poly(methyl methacrylate) and silica mixture. The thermal degradation mechanism of poly(methacrylic acid) found by Sacks *et al.* is very different compared to that of poly(methyl methacrylate). However similar surface reactions were observed in polymer/ceramic mixtures. In general, the results agree with the mechanism proposed by Bakht [4]. Similar work carried out in an oxygen atmosphere showed different results due to oxidative degradation.

Masia *et al.* [8] investigated the effect of various oxides on PVB burnout behavior in air and in argon atmospheres. They found that the oxides used have significant catalytic effects on both thermal and thermal-oxidative degradation of PVB. Masia *et al.* concluded that besides surface chemistry, the surface structure, number of hydroxyl groups, percentage of free water, amount of oxy-

gen adsorbed on the oxide surface and surface impurities would influence binder degradation. Cima *et al.* [11] studies the binder distribution and the effect of different atmosphere on binder degradation.

There is some evidence [12] to indicate that bound water on ceramic surfaces promotes thermal degradation. This effect is significant if the filler surface is hydrophobic (silica, clay, etc.), and the polymer has groups that are sensitive to hydrolysis. Water tightly bound [12] to the filler surface possesses acidic properties which leads both to the acceleration of hydrolysis of the macromolecules and to their acidolysis, especially at elevated temperatures. The recent work of Howard *et al.* [6] sheds some light on the interaction of PVB on alumina surface. They found that low molecular weight PVB's burned cleanly and the hydroxyl and acetate functional groups affected the adsorption of PVB on alumina. They examined the adsorption characteristics using variable-temperature FTIR. Grachev *et al.* [13] carried out spectroscopic studies on the thermal degradation of PVB and found that the degree of substitution of alcohol groups by butyral groups greatly influenced degradation. Yang *et al.* [14] showed that the thermal properties of composites at elevated temperatures can be predicted more accurately if degradation is taken into consideration. In their work, Yang *et al.* proposed a model for predicting the density of laminates as a function of the process variables, lamination temperature, pressure and time. An earlier paper [15] discussed the steam oxidation of carbon left behind due to thermal degradation of polymers in ceramics.

The binder thermal decomposition process involves chemical reactions as well as heat and mass transfer. It is also affected by the substrate's geometry, apparent density, void volume and particles size as well as distribution. Literature review carried out showed a lack of quantitative information on the kinetics of the thermal degradation of polymers in ceramic surfaces. This paper provides quantitative information on the kinetics of thermal degradation of PVB and PVB in alumina, mullite and silica. In addition, this paper also discusses the effect of heating rates and pellet compression pressure on the thermal degradation of PVB in alumina, mullite and silica composites.

Experimental procedure

Thermogravimetric analysis provides valuable information on thermal degradation under constant heating rates and different atmospheres. One can investigate the thermal behavior of ceramic/polymer composites by measuring the weight loss as a function of temperature and time. This data when coupled with an appropriate model for reaction mechanism (listed in Table 2) [16] can be used to interpret and relate the kinetic parameters to physical parameters of the system. For complex systems like binder burn out, this empirical kinetic analysis will not reveal microscopic information but an overall activity within the degradation temperatures.

Three ceramic composites were prepared by using PVB as the binder and, methyl alcohol and methyl isobutyl ketone as solvents. The weight average molecular weight of PVB (Aldrich) was 50.000–75.000 and its glass transition temperature was 65–72°C as measured using a Perkin Elmer DSC 7 Different Scanning Calorimeter. The three ceramic materials were procured form different sources, alumina (5 μm) from IBM, mullite (2–3 μm) form Baikowski International, and silica (5 μm) from U.S. Silica. The ceramics were calcined at 650°C for 24 h and samples were made by mixing the ceramic and the binder in a restricted air flow chamber, then adding the solvent dropwise and finally blending the mixture in a blender. The composition of the mixtures was 85% ceramic and 15% organics including the binder. The composition of the organics was 10% PVB, 20% methyl isobutyl ketone and 70% methanol by weight. A hand operated press (Buehler) was used to make the pellets at different pressures from 4000 to 8000 psig in a single-step change. The pellets were first held at 2000 psig for two minutes and at the desired final pressure for 4 min. After this compression stage, the pellet diameter was 4.8 mm, length about 3 mm and the mass was around 75±5 mg. Densities of the pellets were measured using a modified ASTM D2771-90 method. The properties of the pellets are recorded in Table 1. The pellets were stored in a desiccator till they are used.

Table 1 Properties of the ceramics and ceramic/polymer composites

Ceramic	Particle size/	Surface area/	Bulk density/g cm^{-3}		
Composites	μm	m^2 gm^{-1}	4000 psig	6000 psig	8000 psig
Alumina/PVB	5	1	2.174	2.388	2.391
Mullite/PVB	2–3	2	1.623	1.710	1.720
Silica/PVB	5	5	1.353	1.510	1.526

A Perkin-Elmer TGA 7 equipped with a high temperature furnace was used to measure the weight loss of the binder PVB from 323 to 1273 K, the region where most of the decomposable materials would burn out. A Perkin-Elmer 2000 FTIR system with a resolution of 4 cm^{-1} was infrared with the TGA 7 to identify the evolving gases. Thermogravimetric analysis was carried out in a nitrogen atmosphere at a flow rate of 25 cm^3/min and heating rates of 5, 10 and 20 cm^{-1}. The thermograms were taken for PVB alone, PVB+alumina, PVB+mullite and PVB+silica. The degree of conversion is defined as

$$\alpha(T, t) = \frac{m^{\circ}_{\text{pellet}} - m_{\text{pellet}}(T, t)}{m^{\circ}_{\text{pellet}} - m^{\infty}_{\text{pellet}}} \quad (1)$$

where m°_{pellet} is the initial pellet mass, m^{∞}_{pellet} is the final pellet mass, $m_{pellet}(T, t)$ is the mass of the pellet at any time t, and $\alpha(T, t)\rightarrow 0$ at $t=0$ and $\alpha(T,t)\rightarrow 1.0$ at $t=\infty$.

Data analysis

The irreversible thermal decomposition of solids can be described by the general chemical equation

$$sS_{(s)} \rightarrow rR_{(s)} + vV_{(g)} \tag{2}$$

where S, R and V represent original solids, final solid residue and volatile material respectively and s, r, v are stoichiometric coefficients. The decomposition rate of a solid can be represented by the rate expression

$$\frac{d\alpha}{dt} = kf(\alpha) \tag{3}$$

where α is fraction of solid decomposed at time t, $f(\alpha)$ is a function of α depending on the mechanism and k is the rate constant given by the Arrhenius equation

$$k=A\exp(-E_a/RT) \tag{4}$$

where A is Arrhenius pre-exponential factor, E_a is the activation energy, R is the universal gas constant. For a linear heating rate, $\beta = dT/dt$ and using the Arrhenius equation, the decomposition rate equation can be written in the integral form as

$$\int_{\alpha_o}^{\alpha} \frac{d\alpha}{f(\alpha)} = \frac{A}{\beta}\int_{T_o}^{T} \exp(-E_a/RT)dT \tag{5}$$

or in the differential form as

$$\frac{d\alpha}{dT} = \frac{A}{\beta}\exp(-E_a/RT)\, f(\alpha) \tag{6}$$

Of these two forms, the integral form eliminates the inherent difficulties of the differential form when searching numerically the global minimum of the nonlinear kinetic function. Klyuchnikov *et al.* [17] proposed a computational strategy to prevent the divergence and tried to fit their data to the Arrhenius kinetic parameters. Their results showed that even for a single heating rate the activation energy values could vary from 152 to 226 kJ mol^{-1}, and the order of the reaction from 0.65 to 1.0. Ozawa and Kato [18] developed a method to ex-

Table 2 Commonly used α function for solid state decomposition reactions

Models	$f(\alpha)$	$f(\alpha) = \int d\alpha/f(\alpha)$
1. Coats-Redfern	$(1-\alpha)^n$	$[1-(1-\alpha)^{1-n}]/(1-n)$
Nucleation and nuclei growth		
2. Mampel unimolecular law	$1-\alpha$	$-\ln(1-\alpha)$
3. Two-dimensional growth	$2(1-\alpha)[-\ln(1-\alpha)]^{1/2}$	$[-\ln(1-\alpha)]^{1/2}$
4. Three-dimensional growth	$3(1-\alpha)[-\ln(1-\alpha)]^{1/3}$	$[-\ln(1-\alpha)]^{2/3}$
Diffusion		
5. Parabolic law	α^{-1}	$\alpha^2/2$
6. Valensi equation	$[-\ln(1-\alpha)]^{-1}$	$(1-\alpha)\ln(1-\alpha)+\alpha$
7. Jander equation	$3(-\alpha)^{1/3}/2[(1-\alpha)^{-1/3}-1]$	$[1-(1-\alpha)^{1/3}]^2$
8. Brounshtein-Ginstiling equation	$3/2\cdot[(1-\alpha)^{-1/3}-1]^{-1}$	$1-2/3\alpha-(1-\alpha)^{2/3}$
Phase boundary movement		
9. One-dimensional	constant	α
10. Two-dimensional	$2(1-\alpha)^{1/2}$	$1-(1-\alpha)^{1/2}$
11. Three-dimensional	$3(1-\alpha)^{2/3}$	$1-(1-\alpha)^{1/3}$

tract activation energy values from the derivative thermogravimetric (DTG) data. They showed that a linear plot results when the intensity of the master peak is plotted against reciprocal peak temperature. However, this method is not suitable for a system with two equal intensity DTG peaks. In addition to the differential and Ozawa methods, the kinetic parameters can be evaluated from the integral form by using either an iteration scheme [19] or an integral approximation [20, 21]. Either approach requires the specification of the function $f(\alpha)$. Zsakó and coworkers [19] in a series of papers published in this journal used different $f(\alpha)$ functions (Table 2) and showed that there is an empirical between frequency factors and activation energies. They also noted three degradation regions in their work on cobalt-ethylenediamine pyridine complexes and showed that the Coats-Redfern $f(\alpha)$ function best fitted their data. In this paper we have adopted to integral approach extended by Ma *et al.* [21]. They derived an approximation of integrated form as

$$\log\left[\frac{F(\alpha)}{T^2}\right] = \log\left[\frac{AR}{\beta(E+2RT)}\right] - \frac{E}{2.303RT} \tag{7}$$

where $F(\alpha)$ is the integral form of the function $f(\alpha)$ and $(E+2RT)$ is assumed as a constant for moderate temperatures. A plot of the $\log F(\alpha)/T^2$ *vs.* $1/T$ should

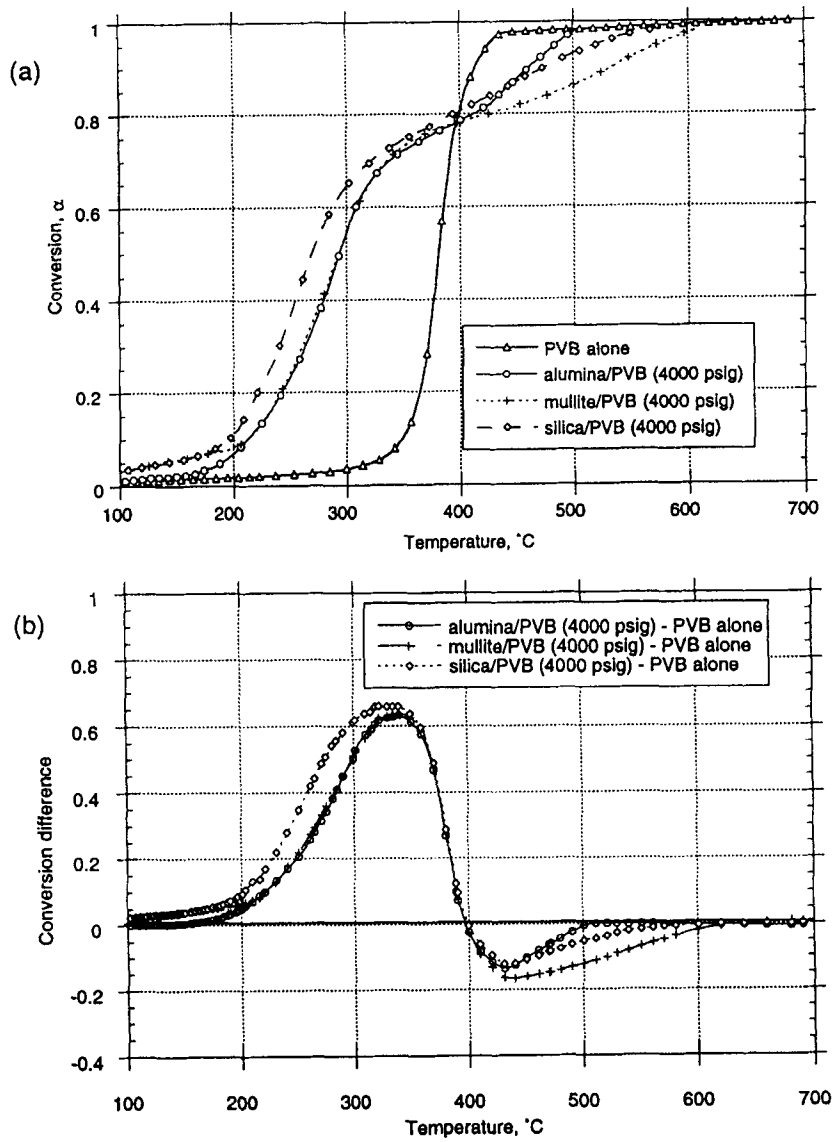

Fig. 1 TG plots of PVB alone, alumina+, mullite+, and silica+PVB pellets decomposed in nitrogen at 5°C min^{-1} (a), and the conversion differences of ceramic/PVB pellets to that of PVB alone (b)

result in a straight line with a slope of $-E/R$ for the correct form of $F(\alpha)$. Cumming [22] and Ma, *et al.* [21] applied this type of analysis to the pyrolysis of coal and found that Arrhenius plots are characterized by two or more regions of

striking linearity, each with its own associated value of apparent activation energy. Therefore, they utilized the concept of a weighted mean apparent activation energy (E_m) to describe the overall degradation process. It is defined as

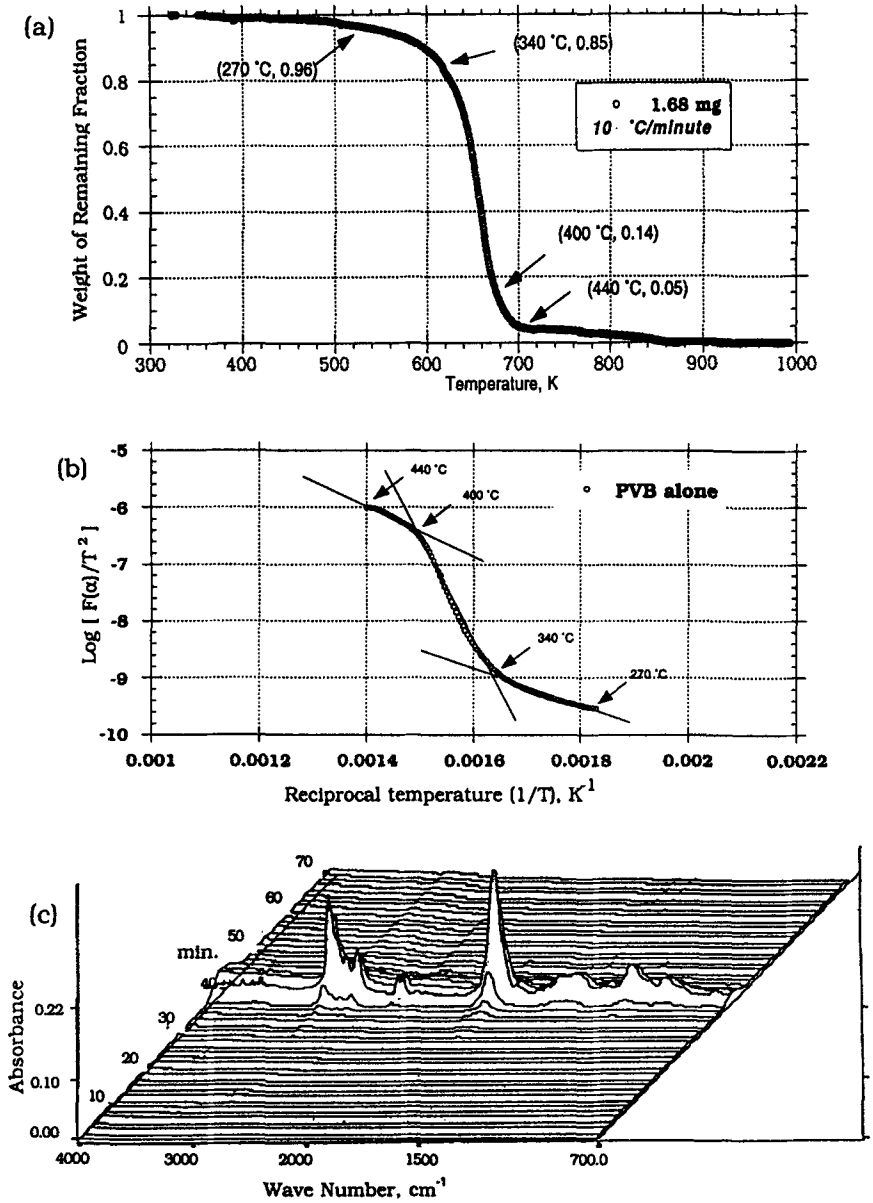

Fig. 2 Results of PVB decomposed at 10°C min^{-1} in nitrogen atmosphere and IR spectra of evolving gases from (a) Thermogravimetric analysis (TG), (b) kinetic function analysis and (c) FTIR interfaced with TG

Table 3 Kinetics results of PVB decomposed in nitrogen atmosphere at different heating rates and different sample weight

PVB powder	Sample weight	Temperature range/°C	Conversion range	E_i/ kJ mol^{-1}	Regression coefficient	E_m/ kJ mol^{-1}
5°C min^{-1}	5.14 mg	271–335	.04–.11	76	.992	
		335–392	.11–.77	274	.991	
		392–429	.77–.95	92	.953	201
5°C min^{-1}	20.37 mg	273–333	.04–.11	78	.994	
		333–401	.11–.83	240	.995	
		401–425	.83–.92	72	.982	185
	20.66 mg	276–330	.04–.09	66	.990	
		330–403	.09–.82	250	.996	
		403–427	.82–.93	84	.997	196
	21.11 mg	263–352	.04–.21	128	.993	
		352–401	.21–.83	276	.997	
		401–422	.83–.94	93	.991	199
10°C min^{-1}	1.68 mg	263–340	.04–.14	82	.993	
		340–402	.14–.84	246	.994	
		402–422	.84–.94	90	.992	189
	20.70 mg	285–359	.04–.21	128	.993	
		359–405	.21–.83	283	.997	
		405–430	.83–.93	66	.947	202
	21.06 mg	287–360	.04–.21	134	.994	
		360–403	.21–.83	283	.997	
		403–430	.83–.93	91	.985	203
20°C min^{-1}	21.71 mg	289–361	.04–.19	126	.998	
		361–407	.19–.78	278	.998	
		407–448	.78–.95	92	.986	198

$$E_m = W_1E_1 + W_2E_2 + ... + W_nE_n \quad (8)$$

where W_1 to W_n are the weighted fractions (which can be determined from the range of conversion), and E_1 to E_n are the individual apparent activation energies related to corresponding regions of Arrhenius linearity. The overall activation energy, E_{ov} was computed as the arithmetic average of the weighted mean apparent activation energy values over the range of pellet compressing pressures. This was done as activation energy values over an entire pressure range

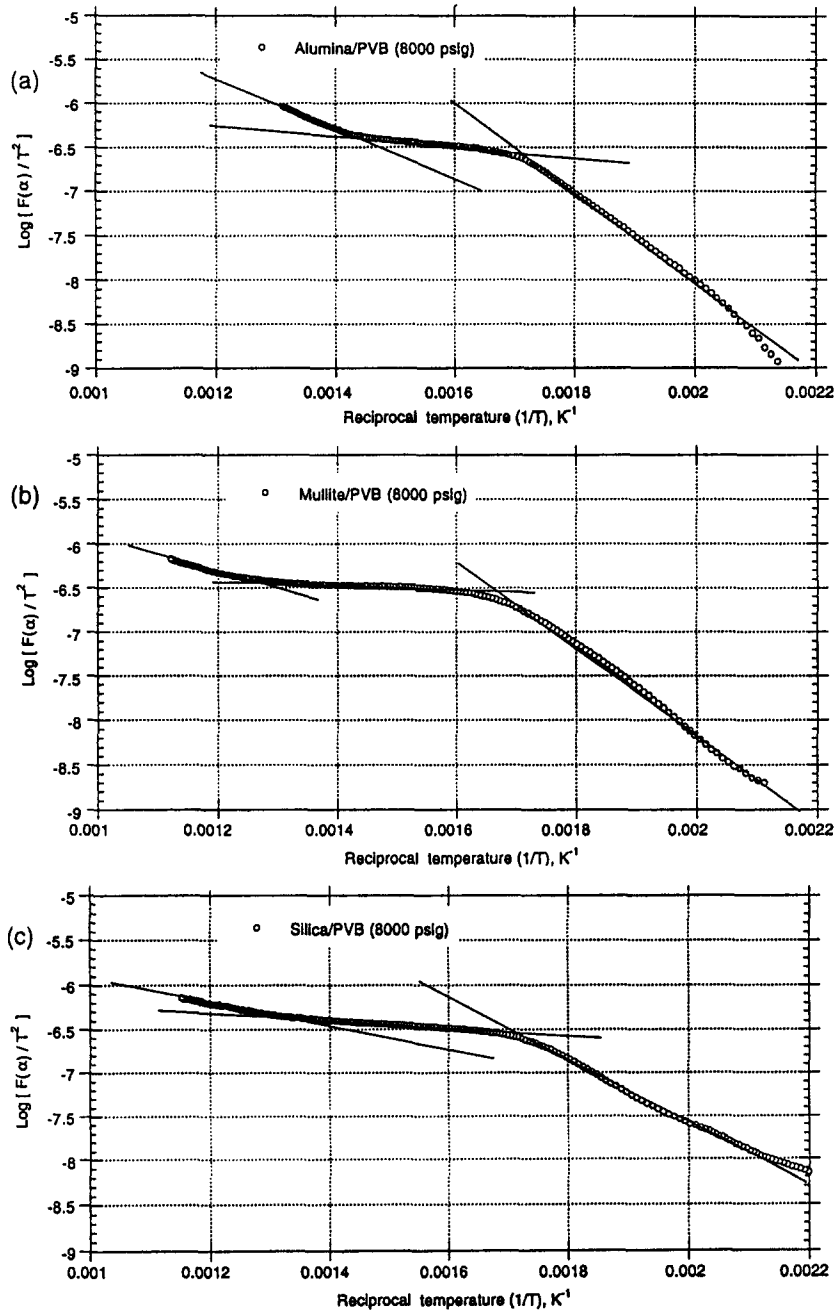

Fig. 3 Plots of kinetics analysis of (a) alumina/PVB, (b) mullite/PVB, and (c) silica/PVB pellets decomposed in nitrogen atmosphere at 5°C min^{-1}

were within ±10%. These results are shown in Tables 3 to 6 and discussed in detail in the next section.

Results and discussion

The thermograms of PVB alone, alumina+, mullite+, and silica+PVB pellets are shown in Fig. 1(a). The decomposition of the polymer in ceramic/polymer composites starts earlier compared to the polymer alone and this could be due to the catalytic effect of the ceramic. The results of Tables 3 to 6 show that the activation energies for each stage of degradation with silica is less than the activation energies either for mullite or alumina. Figure 1(b) shows the conversion difference of ceramic/PVB composites as a function of temperature when subtracted from the conversion of PVB alone. The region above the zero displays the acceleration of the thermal decomposition of the composites and the region below refers to hindered reaction. Silica/PVB composites hold the highest peak and also largest peak area above zero. This reveals that the catalytic properties of silica favour polymer degradation, and this catalytic effect could be due to the acidic nature of silica.

Different $F(\alpha)$ listed in Table 2 were tested with experimental data and the Jander diffusion controlled model was found to be the best to fit the data with the highest regression coefficient ($R > 0.98$) and the lowest standard deviation. Therefore, Jander's model was used to extract the kinetic parameters in this paper. Three linear Arrhenius regions were found in the $\log[F(\alpha)/T^2]$ *vs.* $1/T$ plots for the analysis of thermal degradation data of PVB and PVB/ceramics. Figures 2(a) and 2(b) show the results of thermogravimetric analysis of PVB decomposition. Figure 2(c) shows the 3-Dimensional stacked FTIR spectra of mixture of evolving gases at elevated temperatures. In the case of PVB-alone, the first linearity starts at 270°C and ends at 340°C. The weight loss is only 10%, which agrees with the small effluent IR spectra. The second stage is the main region of thermal degradation of PVB where maximum weight loss (~70%) occurs in the temperature range of 340 to 400°C. In addition, large amount of gases were released at this stage as shown in the FTIR spectra. The major evolving gases were identified as butanoic acid and butanal accompanied with small amounts of butanol and acetic acid. The third stage of degradation starts at 400°C and ends at 440°C. The conversion is about 10% and correspondingly, small amount of gases were released. The results are summarized in Table 3 and include also the effect of sample size and heating rates. The results indicate that both heating rates and sample size do not affect E_m values significantly and these variations maybe well within the experimental error. However heating rates have some effect on the three different stages of degradation in the case of the polymer/ceramic composites as shown in Tables 4 to 6.

Table 4 Kinetic results of PVB in alumina powder and pellets compressed at 4000 and 8000 psig

Heating rate/ °C min^{-1}	Sample	T_{range}/ °C	Conversion range	A_i/ min^{-1}	E_i/ kJ mol^{-1}	Regression coefficient	E_m/ kJ mol^{-1}	E_{ov}/ kJ mol-1
5	powder	172–349	.04–.75	8.8325e+05	89	.996		
		349–419	.75–.84	0.032313	10	.994		
		419–516	.84–.98	6.0060	36	.996	69	
	pellet-4000 psig	181–330	.04–.68	1.6012e+06	91	.998		
		330–418	.68–.81	0.035547	11	.995		
		418–502	.81–.98	41.901	46	.992	68	
	pellet-8000 psig	192–329	.04–.69	8.6306e+06	97	.995		
		327–420	.69–.83	0.056549	13	.997		
		420–489	.83–.98	151.44	53	.998	72	70
10	powder	179–372	.04–.76	3.0727e+05	83	.997		
		372–441	.76–.84	0.040671	8	.992		
		441–519	.84–.98	89.617	46	.993	67	
	pellet-4000 psig	206–388	.04–.78	1.8849e+06	95	.998		
		388–460	.78–.85	0.035284	8	.995		
		461–564	.85–.98	3.6511	31	.982	75	
	pellet-8000 psig	203–349	.04–.71	1.3907e+07	99	.995		
		349–430	.71–.83	0.087053	12	.994		
		431–505	.83–.97	68.363	46	.997	74	72
20	powder	244–390	.09–.84	3.3783e+07	107	.993		
		390–515	.84–.94	0.052568	5	.996		
		515–572	.94–.98	1.5299	22	.991	81	
	pellet-4000 psig	205–393	.03–.82	9.5290e+07	113	.992		
		393–493	.82–.91	0.070990	7	.997		
		493–573	.91–.98	2.2019	24	.995	92	
	pellet-8000 psig	224–389	.05–.83	1.3780e+08	113	.992		
		389–513	.83–.93	0.094859	8	.999		
		513–576	.93–.98	2.5611	25	.997	90	88

Table 5 Kinetic results of PVB in mullite powder and pellets compressed at 4000 and 8000 psig

Heating rate/ °C min^{-1}	Sample	T_{range}/ °C	Conversion range	A_i/ min^{-1}	E_i/ kJ mol^{-1}	Regression coefficient	E_m/ kJ mol^{-1}	E_{ov}/ kJ mol^{-1}
5	powder	184–343	.07–.74	2.0788e+05	82	.994		
		343–522	.74–.88	0.0075165	4	.993		
		522–620	.88–.98	1.3482	32	.99	58	
	pellet-4000 psig	175–352	.08–.73	9.9900	79	.992		
		352–500	.73–.86	0.0075045	4	.994		
		500–609	.86–.98	1.1047	30	.991	56	
	pellet-8000 psig	200–355	.06–.72	5.7264e+05	86	.991		
		355–512	.72–.87	0.014009	7	.993		
		512–618	.87–.98	1.2655	31	.991	61	58
10	powder	171–369	.05–.77	2.2418e+05	79	.990		
		369–515	.77–.88	0.012201	3	.984		
		515–613	.88–.98	1.8867	29	.981	60	
	pellet-4000 psig	171–360	.05–.73	4.9174e+05	82	.990		
		360–501	.73–.86	0.013346	4	.980		
		501–606	.86–.98	3.7051	33	.990	61	
	pellet-8000 psig	175–367	.05–.77	2.8905e+05	81	.993		
		367–566	.77–.93	0.028410	6	.992		
		566–628	.93–.98	2.4508	31	.981	61	61
20	powder	170–336	.05–.72	2.2901e+06	87	.990		
		336–475	.72–.86	0.037314	5	.982		
		475–580	.86–.98	6.0899	31	.990	62	
	pellet-4000 psig	171–363	.04–.78	7.1789e+05	84	.992		
		363–576	.78–.96	0.092910	8	.992		
		576–622	.96–.98	1.1448	22	.987	64	
	pellet-8000 psig	178–408	.04–.86	5.2583e+05	82	.990		
		408–528	.86–.93	0.19526	12	.985		
		528–618	.93–.98	0.21534	12	.987	68	65

Table 6 Kinetics results of PVB in silica powder and pellets compressed at 4000 and 8000 psig

Heating rate/ °C	Sample	T_{range}/°C	Conversion range	A_i/ 1 min^{-1}	E_i/ kJ mol^{-1}	Regression coefficient	E_m/ kJ mol^{-1}	E_{ov}/ kJ mol-1
5	powder	180–325	.08–.69	2.4733e+05	78	.997		
		325–440	.69–.83	0.019337	8	.997		
		440–560	.83–.94	0.11588	15	.993	50	
	pellet-4000 psig	190–311	.09–.65	1.1141e+06	84	.998		
		311–440	.65–.83	0.029647	10	.995		
		440–506	.88–.90	0.13623	16	.996	50	
	pellet-8000 psig	180–315	.10–.64	8084.2	65	.999		
		315–467	.64–.83	0.019860	8	.994		
		467–608	.83–.95	0.089853	14	.991	38	46
10	powder	190–300	.10–.65	5.9078e+06	89	.999		
		300–400	.65–.80	0.10858	12	.988		
		400–560	.80–.94	0.11258	11	.997	52	
	pellet-4000 psig	186–300	.08–.57	6.0305e+05	81	.999		
		300–440	.57–.80	0.068009	11	.983		
		440–620	.80–.96	0.21548	15	.993	45	
	pellet-8000 psig	194–370	.08–.69	12876	68	.999		
		370–560	.69–.84	0.013088	3	.978		
		560–725	.84–.97	0.53790	22	.992	45	47
20	powder	195–365	.07–.70	38619	69	.998		
		365–720	.70–.90	0.028325	–	–		
		720–882	.90–.98	0.37733	15	.990	45	
	pellet-4000 psig	190–330	.08–.64	3.3316e+05	78	.998		
		330–470	.64–.82	0.070116	8	.992		
		470–635	.82–.97	0.54936	17	.994	48	
	pellet-8000 psig	195–370	.06–.69	1.6493e+05	76	.999		
		370–684	.69–.88	0.027420	–	–		
		684–884	.88–.98	0.53228	17	.992	50	48

Figure 3 shows a typical plot of the $\log[F(\alpha)/T^2]$ *vs.* $1/T$ for the degradation of PVB in alumina, mullite and silica with composites made at 8000 psig. Similar results were observed at 4000 psig compression pressure and for the powder. A comparison of the results for PVB alone and for PVB in ceramics shows that

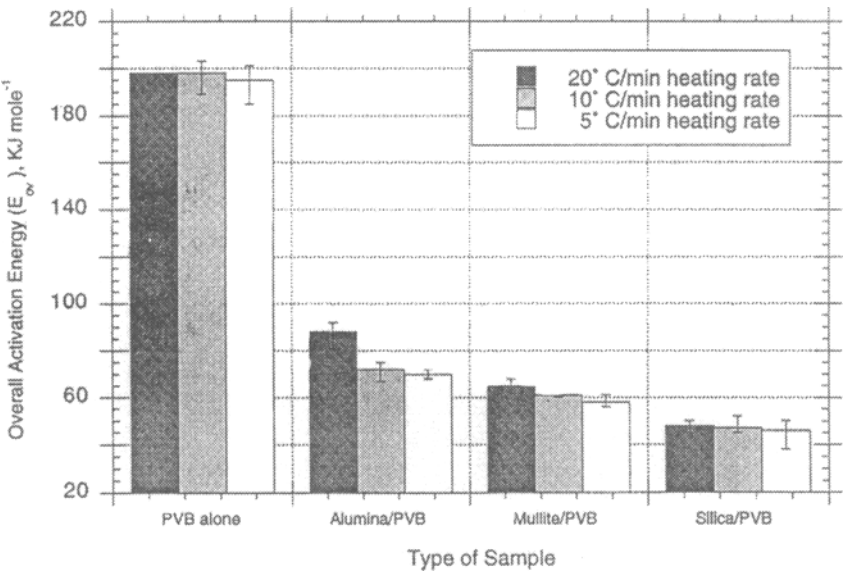

Fig. 4 Plots of overall apparent mean activation energy *vs.* different heating rates and materials, where ■ represent heating rate 20°C min^{-1}, ⊠ 10°C min^{-1} and □ 5°C min^{-1}

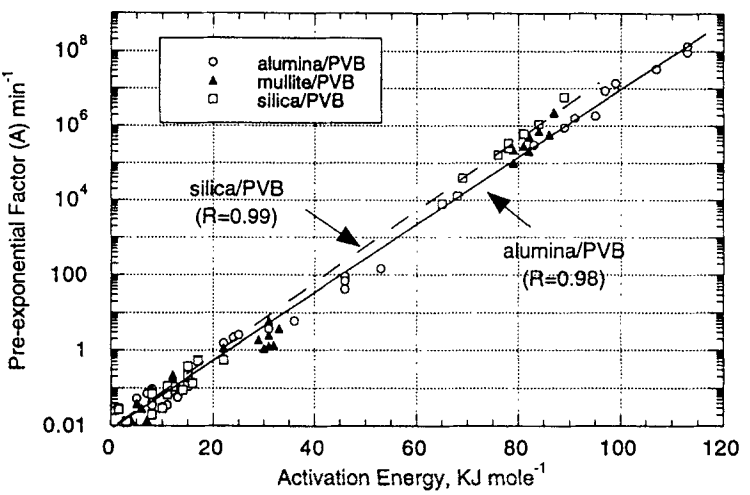

Fig. 5 Plots of the activation energy *vs.* the logarithm of preexponential constant for the case of PVB/alumina, PVB/mullite and PVB/silica

major degradation in the case of PVB/ceramics occurs in the first stage which ends around 340°C whereas in the case of PVB alone major degradation occurs during the second stage which starts around 340°C. This clearly points to the catalytic effect of the ceramics. The values of the activation energies during these stages suggest that the primary stage is dominated by chemical decomposition processes.

Tables 4 to 6 show the kinetic parameters of the powder form and pellet forms collected along with heating rates, temperature range, conversion and regression coefficient. Also listed in these tables are activation energies, E_m, determined by Eq. (8). Figure 4 shows the overall activation energies at different heating rates for all the samples. These results indicate that heating rates have little effect and the overall activation energies progressively decrease from pure PVB to PVB/silica composites. However for the same ceramic+PVB, E_{ov} values increase by a small percentage with increase in heating rates. This increase may be due to the sample thermal lag and the reduction of equilibrium rates at higher heating rates, and indicates also that there is no change in the mechanism of thermal degradation with heating rates. Figure 5 shows the plot of Arrhenius pre-exponential factor (A_i) *vs.* its associated activation energies (E_i). As E_i increases, A_i also increases and *vice versa*. The nature of the changes of Arrhenius constant depending on the changes of activation energies has been characterized as the kinetic compensation effect. It is found that this correlation can be valid not only for different heating rates, but also for different packing conditions.

Conclusions

This paper presents the kinetics of thermal degradation of polymers in ceramic surfaces and, the effect pellet compression pressure and heating rates. This study is important in tape casting where multiple layers of ceramics tapes are laminated and sintered for use in various applications such as high end computers, manufacture of heat exchangers, turbine blades, etc. This paper also presents results of thermal degradation of powder and pellets made at different pressures. Non-isothermal data provides a rapid way of obtaining the kinetics of degradation.

References

1 K. Niwa et al., 'Multilayer Ceramic Circuit Board with Copper Conductor', Multilayer Ceramic Devices, Editors: J. B. Blum and W. R. Cannon, Adv. Ceramics, 19 (1986) 41.
2 R. R. Tummala, J. Am. Ceram. Soc., 74 (1991) 895.
3 P. Bataille and B. T. Van, J. Thermal Anal., 8 (1975) 141.
4 M. F. Barkht, Pak. J. Sci. Ind. Res., 26 (1983) 35.
5 W. K. Shih et al., 'Pyrolysis of Poly(Vinyl Butyral) Binders; I, Degradation Mechanism,' p. 549 in Ceramic Transactions, Vol I., Ceramic Powder Science, IIA. Edited by G. L. Messing et al. Am. Ceram. Soc. Westerville, OH, 1988.

6 K. E. Howard et al., J. Am. Ceram. Soc., 73 (1990) 2543.
7 Y. N. Sun et al., 'Pyrolysis Behavior of Acrylic Polymers and Acrylic Polymer/Ceramic Mixtures,' pp. 538 in Ceramic Transactions, Vol I., Ceramic Powder Science, IIA. Edited by G. L. Messing et al., Am. Ceram. Soc., Westerville, OH, 1988.
8 S. Masia et al., J. Material Sci., 24 (1989) 1907.
9 G. W. Scheiffele and M. D. Sacks, 'Pyrolysis of Poly/Vinyl Butyral) Binders: I Degradation Mechanism', p. 559 in Ceramic Transactions, Vol I., Ceramic Powder Science, IIA. Edited by G. L. Messing et al., Am. Ceram. Soc., Westerville, OH, 1988.
10 A. A. Parker et al., J. Appl. Polymer Sci., 48 (1993) 1701.
11 M. J. Cima et al., 'Firing-Atmosphere Effects on Char Content from Alumina-Polyvinyl Butyral Films', p. 567 in Ceramic Transactions, Vol. I., Ceramic Powder Science, IIA. Edited by G. L. Messing et al., Am. Ceram. Soc. Westerville, OH, 1988.
12 M. T. Bryk, Degradation of Filled Polymers High Temperature and Thermal-Oxidative Processes, Ellis Horwood, New York, NY, 1991.
13 V. I. Grachev et al., A Spectroscopic Study of the Kinetics of Thermal Oxidative Degradation of Poly(vinyl butyral), Vysokomol. Soyed. A16:2 (1974) 317.
14 T. C. Yang et al., Heat Capacity of Composites of Alumina, Mullite and Silica, presented at The Polymer processing Society Meeting, West Virginia University, Morgontown, WV, August (1993).
15 M. V. Boddu et al., J. Am. Ceram. Soc., 73 (1990) 1701.
16 C. H. Bamford and C. F. H. Tipper, Reactions in Solid State, Elsevier Scientific, New York, NY, 1980, p. 74.
17 V. N. Klyuchnikov et al., Polymer Sci. U.S.S.R., 31 (1989) 735.
18 T. Ozawa and T. Kato, J. Thermal Anal., 37 (1991) 1299.
19 J. Zsakó and J. Zsakó, Jr., J. Thermal Anal., 19 (1980) 333.
20 T. V. Lee and S. R. Beck, AIChE J., 30 (1984) 517.
21 S. Ma et al., J. Thermal Anal., 37 (1991) 1161.
22 J. W. Cumming, Fuel, 63 (1984) 1436.